

Reliability and Thermal Stability of MoS₂ FETs with Ultrathin CaF₂ Insulators

Yu.Yu. Illarionov^{1,2}, A.G. Banskchikov², D.K. Polyushkin¹, S. Wachter¹, M.I. Vexler², N.S. Sokolov², T. Mueller¹, T. Grasser¹
¹TU Wien, Vienna, Austria ²Ioffe Institute, St-Petersburg, Russia

Two-dimensional (2D) materials can potentially provide a route to overcome the limitations of Si technologies by enabling nanoscale more than Moore FETs. Fabrication of these devices requires *i)* 2D semiconductors with sizable bandgaps and high carrier mobilities and *ii)* competitive insulators to separate the channel from the gate. However, up to now attention has been mostly paid to the channel materials, while insulators fully suitable for 2D FETs have not been identified. For instance, native oxides of 2D semiconductors, which would go along with them as well as SiO₂ goes with Si, either do not exist or cannot be easily synthesized. As a result, 2D FETs currently face the same problems as many other emerging technologies (e.g. Ge, III-V or GaN FETs), and commercial devices do not yet exist.

The absence of native insulators for 2D FETs requires the use of other materials. The most obvious of them are oxides known from Si technologies (e.g. SiO₂, Al₂O₃, HfO₂), which have been used in most 2D FETs. However, despite a respectable performance of some devices, the typical thickness of the oxides used ranges from tens to even hundreds of nanometers. When being scaled down to the equivalent oxide thicknesses (EOT) below 1nm, as required for end-of-the-roadmap devices, these oxides become amorphous. Thus, their interfaces with 2D channels are of poor quality and contain numerous defects which degrade the performance and reliability of 2D FETs. Another solution is the use of 2D insulators which form well-defined van der Waals interfaces with 2D channels. The best known of them is hBN which indeed resulted in the improvement of 2D FETs. However, when scaled down to several nanometers thickness, hBN exhibits significant tunnel leakage currents. This is due to the moderate dielectric properties ($\epsilon < 5$, $E_G = 6$ eV) of hBN, which appears to be unsuitable for scaling. As for other 2D insulators, such as mica or oxide nanosheets, their usability in devices has not been demonstrated.

As an alternative, we have recently suggested to use calcium fluoride (CaF₂) as an insulator for 2D devices [1]. Few-nanometers thin CaF₂ layers can be grown on Si(111) by molecular beam epitaxy (MBE) which forms an F-terminated inert surface with no dangling bonds [2]. This results in a quasi van der Waals interface with 2D materials (Fig.1a), similar to those formed by hBN. Furthermore, due to its good dielectric properties ($\epsilon = 8.43$, $E_G = 12.1$ eV), the tunnel currents through CaF₂ are lower than for most high-k oxides with equal EOT, not to mention SiO₂ and hBN.

We fabricated hundreds of CVD-grown MoS₂ FETs with epitaxial CaF₂ insulators of record-small thickness of only about 2 nm (EOT less than 1nm), see Fig.1b. The gate currents in our devices are small compared to the drain current (Fig.1c). Thus, already in the first bare channel prototypes we achieve competitive on/off current ratios of up to 10⁷ and SS down to 90 mV/dec (Fig.2a). At the same time, the hysteresis in our devices is even smaller than in Al₂O₃ encapsulated SiO₂(25nm)/MoS₂ FETs [3] (Fig.2b). In Fig.2c we compare the hysteresis widths normalized by the insulator field factor $\Delta V_G/d_{\text{ins}}$, where ΔV_G is the width of the gate voltage sweep range and d_{ins} the insulator thickness. For CaF₂ the hysteresis is comparable to that in Si/high-k FETs.

In Fig.3 we show the results for bias-temperature instabilities (BTI) in our CaF₂(2nm)/MoS₂ FETs. The negative BTI (NBTI, Fig.3a) and positive BTI (PBTI,

Fig.3b) at insulator fields which are typically used for 2D FETs (2.5 to 5MV/cm) are relatively weak. This is likely due to the lack of insulator defects in the crystalline CaF₂ insulator. However, PBTI stress at the insulator field of 7.5MV/cm leads to a negative drift of the threshold voltage (Fig.3c). This kind of degradation has never been observed for 2D FETs with thick insulators, which routinely operate at lower insulator fields. Recently we found that the negative V_{th} shift after PBTI stress observed in our CaF₂/MoS₂ FETs is very similar to that in MoS₂ FETs with 4nm thick hBN insulators [4]. Thus, we suggest that this is due to the activation of breakdown mechanisms in ultrathin insulators. However, we note that a reasonable on current in our CaF₂/MoS₂ FETs can be achieved already at a gate voltage of 1V (F_{ins} of 5MV/cm), allowing safe device operation.

We also analyzed the thermal stability of our devices and found that it strongly depends on the quality of the MoS₂ channel. If the CVD-grown MoS₂ film is formed by few nanometers sized grains (Process 1, Fig.4a), baking of the devices at 100°C introduces a strong hysteresis (Fig.4b). However, this hysteresis is observed only when using small sweep times t_{sw} and disappears for slow sweeps (Fig.4c). We suggest that the origin of this behavior is thermally enhanced creation of S vacancies in MoS₂. These S vacancies can cause a hysteresis when interacting with adsorbates [5], which can penetrate to the CaF₂/MoS₂ interface through the numerous grain boundaries in the small grain MoS₂. In contrast to charge trapping by slow insulator defects, which seems to be missing in CaF₂, interaction between S vacancies and adsorbates is a fast process. This explains the fast sweep hysteresis which we observe. In contrast, in the CaF₂/MoS₂ FETs with larger grains of the MoS₂ film (Process 2, Fig.5a) the hysteresis remains small even after baking at 165°C (Fig.5b), though a negative shift of V_{th} attributed to the creation of S vacancies is present. However, these S vacancies remain passive, since the number of grain boundaries in large grain MoS₂ is small and thus the penetration of adsorbates to the interface is less efficient. At the same time, the number of active defects in crystalline CaF₂ is small, independently of the MoS₂ quality. Thus, the hysteresis in our Process 2 devices remains small within the whole range of sweep times, while being smaller than in Al₂O₃ encapsulated SiO₂(25nm)/MoS₂ FETs (Fig.5c).

In summary, we examined the reliability and thermal stability of the MoS₂ FETs with CaF₂ insulators of record small 2nm thickness. We found that the virtually defect-free nature of CaF₂ insulators leads to a small hysteresis and BTI, while the thermal stability of our devices strongly depends on the quality of the MoS₂ channel.

- [1] Yu.Yu. Illarionov *et al.*, "Ultrathin calcium fluoride insulators for two-dimensional field-effect transistors", *Nature Electron.*, 2019.
- [2] A. Koma *et al.*, "Heteroepitaxy of a two-dimensional material on a three-dimensional material", *Appl. Surf. Sci.*, vol. 41, 451–456, 1990.
- [3] Yu.Yu. Illarionov *et al.*, "Improved Hysteresis and Reliability of MoS₂ Transistors with High-Quality CVD Growth and Al₂O₃ Encapsulation", *IEEE Electron Device Lett.*, vol. 38, 1763–1766, 2017.
- [4] Yu.Yu. Illarionov *et al.*, "Reliability of scalable MoS₂ FETs with 2 nm Crystalline CaF₂ Insulators", *2D Mater.*, 2019.
- [5] A. Di Bartolomeo *et al.*, "Hysteresis in the transfer characteristics of MoS₂ transistors", *2D Mater.*, vol. 5, 015014, 2017.

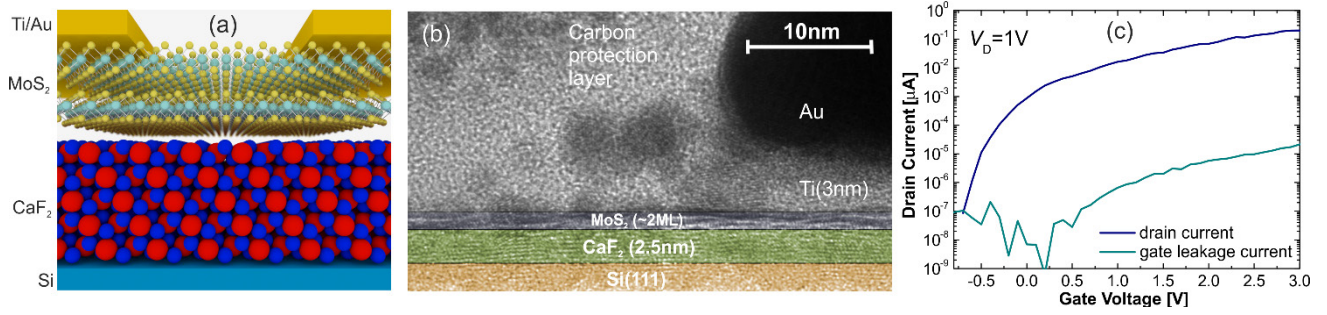


Fig.1. (a) Schematic device layout. (b) TEM image of the channel area. (c) Drain current and gate leakage current vs. gate voltage.

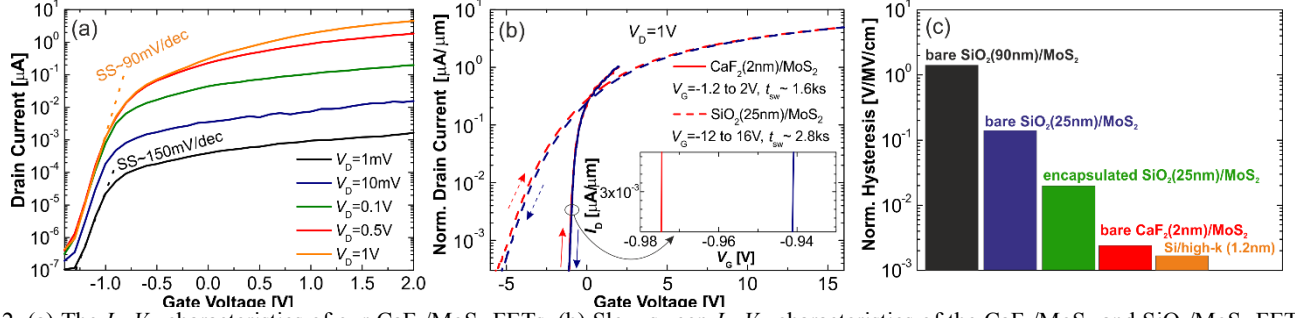


Fig.2. (a) The I_D - V_G characteristics of our $\text{CaF}_2/\text{MoS}_2$ FETs. (b) Slow sweep I_D - V_G characteristics of the $\text{CaF}_2/\text{MoS}_2$ and $\text{SiO}_2/\text{MoS}_2$ FETs. (c) Comparison of the hysteresis width normalized by the insulator field factor for different MoS_2 FETs and Si/high-k devices.

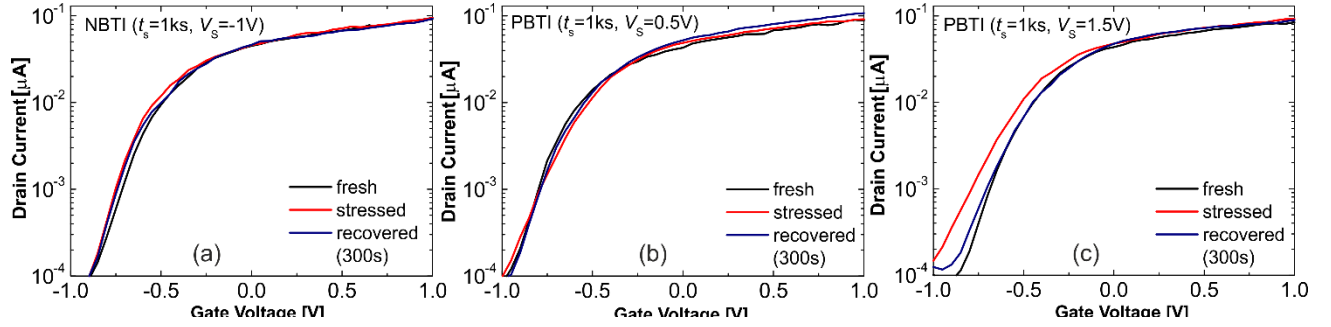


Fig.3. NBTI (a) and PBTI (b,c) in our $\text{CaF}_2/\text{MoS}_2$ FETs. A negative V_{th} shift (c) appears after PBTI stress at $V_g=1.5\text{V}$ ($F_{ins}=7.5\text{MV/cm}$).

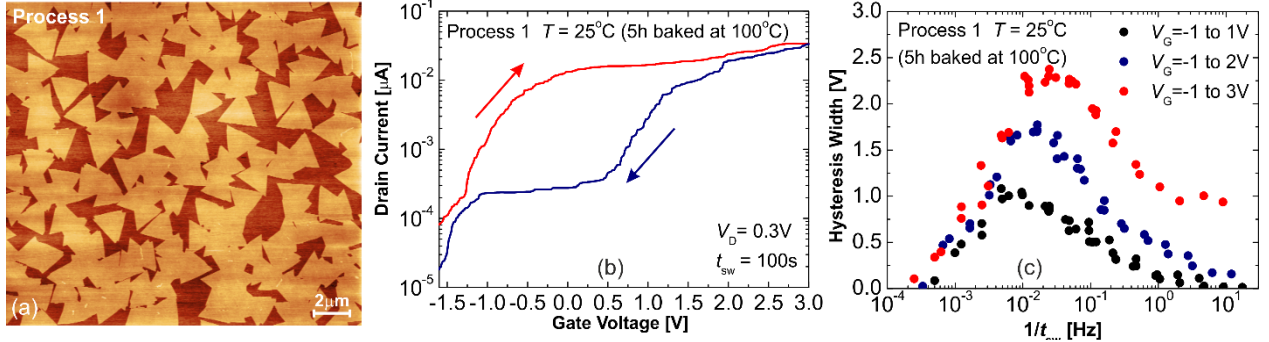


Fig.4. (a) AFM image of the Process 1 MoS_2 film. Fast sweep hysteresis (b) and $\Delta V_H(1/t_{sw})$ dependences (c) after baking at 100°C .

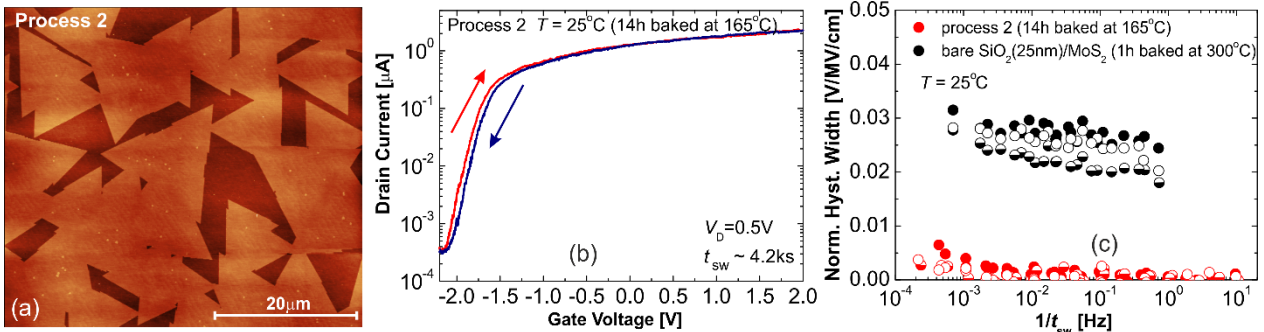


Fig.5. (a) AFM image of the Process 2 MoS_2 film. (b) Slow sweep hysteresis after baking at 165°C . $\Delta V_H(1/t_{sw})$ dependences for the Process 2 $\text{CaF}_2/\text{MoS}_2$ and bare channel $\text{SiO}_2/\text{MoS}_2$ FETs measured after baking (3 devices for each case).